Monitoring Molecular Beacon DNA Probe Hybridization at the Single-Molecule Level

Gang Yao,[a] Xiaohong Fang,[a] Hiroaki Yokota,[b] Toshio Yanagida,[b] and Weihong Tan*[a]

Abstract: We have monitored the reaction dynamics of the DNA hybridization process on a liquid/solid interface at the single-molecule level by using a hairpin-type molecular beacon DNA probe. Fluorescence images of single DNA probes were recorded by using total internal reflection fluorescence microscopy. The fluorescence signal of single DNA probes during the hybridization to individual complementary DNA probes was monitored over time. Among 400 molecular beacon DNA probes that we tracked, 349 molecular beacons (87.5%) were hybridized quickly and showed an abrupt fluorescence increase, while 51 probes (12.5%) reacted slowly, resulting in a gradual fluorescence increase. This ratio stayed about the same when varying the concentrations of cDNA in MB hybridization on the liquid/surface interface. Statistical data of the 51 single-molecule hybridization images showed that there was a multistep hybridization process. Our results also showed that photostability for the dye molecules associated with the double-stranded hybrids was better than that for those with the single-stranded molecular beacon DNA probes. Our results demonstrate the ability to obtain a better understanding of DNA hybridization processes using single-molecule techniques, which will improve biosensor and biochip development where surface-immobilized molecular beacon DNA probes provide unique advantages in signal transduction.

Keywords: fluorescent probes · hybridization · molecular beacons · single-molecule studies · total internal reflection fluorescence microscopy

Introduction

In the past decade, single-molecule detection (SMD) and imaging techniques have made significant advancements not only in ultrasensitive detection, but also in practical applications such as gene chips and in fundamental molecular mechanism studies.[1–8] SMD offers a way to study and characterize detailed physical and chemical properties of individual molecules. SMD can directly observe the stochastic time dependence of molecular behavior, explicitly remove the average effect of the population, and clearly analyze the dynamic process of a biochemical reaction.[9–13] SMD has led to better understandings of molecular mechanisms and to technological advancements in bioanalysis and in biotechnology. The challenge for SMD using fluorescence techniques is to extract fluorescence signals of single molecules from the background noise. Many strategies have been developed to increase the signal-to-noise ratio to achieve SMD.[1,2,4,5,7,14,15] Total internal reflection fluorescence microscopy (TIRFM) is an elegant optical technique that is used to observe single molecule fluorescence at surfaces and interfaces. This technique has been applied to observe single ATP turnover reactions,[2] to study the electrostatic trapping of protein molecules at a solid–liquid interface,[6] and to image conformational dynamics and adsorption/desorption behavior of individual DNA molecules.[16] We have used a single-molecule fluorescence microscope to visualize single actin filaments,[2] to image single DNA probes,[17] to observe single-molecule generation from a chemical reaction on a surface,[7] and to reveal the binding of individual cyclic adenosine 3′,5′-monophosphate molecules to heterotrimeric guanine nucleotide-binding protein coupled receptors on the surface of living cells.[8] Herein, we report the monitoring of the DNA hybridization process at the single-molecule level by using a TIRFM-SMD system and molecular beacon DNA probes.

[a] Prof. Dr. W. Tan, Dr. G. Yao, Dr. X. Fang
Center for Research at the Interface of Bio/nano
Department of Chemistry and the McKnight Brain Institute
University of Florida, Gainesville, Fl 32611 (USA)
Fax: (+1) 352-846-2410
E-mail: tan@chem.ufl.edu

[b] Dr. H. Yokota, Prof. T. Yanagida
Single Molecule Processes Project
Osaka University, Senba-Higashi, 2-4-14
Mino,Osaka 562-0035 (Japan)

DOI: 10.1002/chem.200304977

Molecular beacon DNA probes are attracting increasing attention and are providing a variety of exciting opportunities in DNA and protein studies.[18–23] Molecular beacons (MBs) are a new class of single-stranded oligonucleotide probes that possess a stem-and-loop structure (Figure 1).

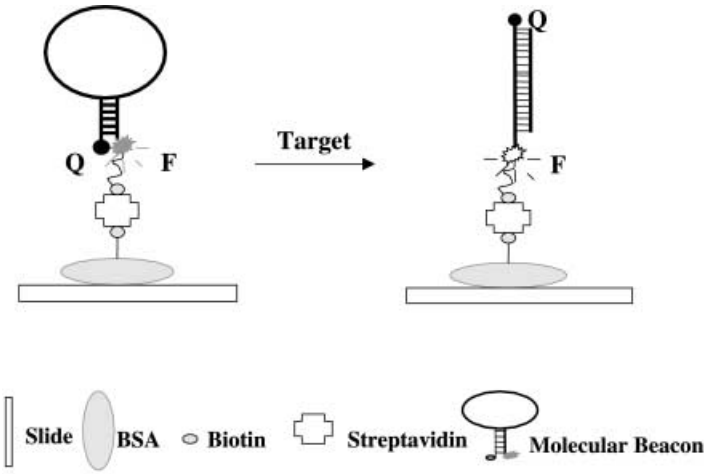

Figure 1. A schematic of the surface-immobilized MB hybridization with cDNA.

The loop portion of a MB is complementary to a target single-stranded DNA, while the stem is formed by five-to-seven base pairs from two complementary arm sequences that are on either side of the MB. A fluorophore is attached to the end of one arm, and a quencher is attached to the other end of the other arm. The stem keeps these two moieties in close proximity, causing the fluorescence to be quenched by energy transfer. When a MB hybridizes with its complementary DNA (cDNA), the beacon undergoes a spontaneous conformational reorganization with the opening of the stem, leading to a fluorescence restoration. The built-in fluorescence signal transducation mechanism provides the molecule beacons many advantages over other DNA probes in selectivity and sensitivity. These unique properties also make molecular beacons suitable probes for the study of the DNA hybridization process, as their fluorescence is a direct indicator of the MBs conformation during hybridization. We have recently developed a surface-immobilizable MB,[21] which makes it possible to monitor individual MBs in the course of hybridization after the MBs are immobilized onto a surface.

Herein, we discuss the monitoring of the DNA hybridization process at the single-molecule level. A biotinylated MB was immobilized on the surface of a quartz slide through biotin–avidin binding. The MB molecules are excited with an evanescent wave field produced by a quartz prism, while the cDNA solution is introduced. Time-lapse fluorescence images of the surface hybridization progression were obtained by a fluorescence microscope equipped with an intensified charge couple device (ICCD). In this way the hybridization kinetics of single DNA molecules as well as the photochemical properties of DNA probes have been studied.

Experimental Section

Reagents: Biotin-labeled tetramethylrhodamine (TMR) and streptavidin were purchased from Molecular Probes (Eugene, OR). The biotinylated MB was custom-designed and synthesized by TriLink Biotechnologies (San Diego, CA), and the cDNA probe was purchased from Integrated DNA Technologies Inc (Coralville, IA). The MB sequence was 5′-biotin TTT TTT TTT T (dC-C6-NH-TMR)-C ACG CTG GAT TAA GAT TGC TGC GTG G-(DABCYL)-3′. The sequence of the cDNA was 5′-CCA CGC AGC AAT CTT AAT CCA-3′. All other reagents such as biotin BSA, streptavidin, and Tris were purchased from Sigma (St. Louis, MO) and used without further purification. Deoxygenated Tris-HCl buffer (pH 8.0, 20 mM Tris-HCl and 3 mM $MgCl_2$) and deoxygenated ultrapure water (>18.3MΩ cm) were used in all experiments described herein.

Sample preparation: A cover glass and a quartz glass slide were used to form a sandwich-like channel, which allows easy introduction of the solution and reproducible control of the hybridization reaction conditions. This reaction sandwich-like channel is similar to what we reported previously.[24] Freshly prepared MB (100 pM or 100 pM TMR, or the mixture of 100 pM MB and 100 nM cDNA) was immobilized on the slide through biotin–avidin interactions. The quartz slide was pretreated with a thin layer of uniform avidin molecules for the subsequent immobilization of the biotinylated MB. A biotin–BSA solution (15 μL, 1.5 mg per mL) was first introduced into the channel. The solution was retained there for 5 min, followed by streptavidin (20 μL, 0.25 mg per mL) for 5 min, and then a biotin–MB (20 μL, 100 pM) for 5 min. Between each procedure, we used Tris-HCl buffer (50 μL) to flush the channel three times to remove the unreacted chemicals. After the sample was placed on the microscope, cDNA (10 μL, 100 nM) was injected into the channel, and the fluorescence images were monitored immediately. The cDNA concentration was also varied (between 50 nM and 500 nM) to test the ratios of slow hybridization versus fast hybridization (see below). For the photobleaching time study, a MB–cDNA duplex was prepared by mixing the MB (100 pM) with cDNA (100 nM) for 30 min in the dark at room temperature, and denatured MB was prepared by heating the MB (1 nM) at 100 °C for 15 min and immediately diluting the denatured MB to 100 pM with 0 °C Tris-HCl buffer solution. After the immobilization of the MB or the duplex on the slide, the channel was also flushed with buffer (50 μL, three times).

Instrumentation: The single-molecule fluorescence experiments were performed by using a total internal reflection (TIR) wide-field microscope as previously described.[2,25] A quartz dove prism was mounted above the microscope objective of an inverted microscope (IX70, Olympus). The sample channel was placed on the microscope stage and set between the prism and the microscope objective. The upper channel of the quartz slide was attached to the prism by a drop of glycerol. A laser beam (514 nm) was produced from an Innova I307C ion laser (Coherent, Santa Clara, CA) with the aperture setting at position 1. After passing through a quarter-wave plate (CVI, Putnam, CT), the laser light was directed to the prism with several optical mirrors and a 12 cm focal length lens. The focusing spot was on the bottom surface of the quartz slide. With the incident angle of the laser beam adjusted to about 70°, TIR took place at the interface between the quartz slide and the sample solution. The evanescent field was used to excite the MB molecules immobilized on the slide surface. The emission signal was collected by an oil-immersion objective (100×, 1.35 NA, UPlanApo, Olympus) and directed to an ICCD camera (Pentamax EEV 512×512 FT, Pentamax, Princeton Instruments), controlled by WinView software (Roper Scientific), for single-molecule imaging. One long-pass filter (550 nm, Chroma, Brattleboro, VT) and one band-pass filter (580DF30, Omega Optics, Brattleboro, VT) were put before the ICCD to select the desired fluorescence signal. The exposure time was set at 100 ms. The laser power at the prism was adjusted to 0.28 $KW\,cm^{-2}$.

Single-molecule monitoring: The experiment was performed in a clean and dark room. A small area in the corner of the sample channel was used to adjust the focusing of the system, and the slide was then moved to the sample section for fluorescence imaging. Single-molecule fluorescence images were recorded with the ICCD camera continuously over a small area (200 pixel×200 pixel, 44 μm×44 μm). From these consecutive

images, time traces of fluorescence emission were constructed by analyzing a 28-pixel area (1.36 μm^2) with Image J software (NIH) and a self-developed computation program.

Results and Discussion

Single-molecule (SM) imaging: To monitor the dynamics of individual molecules during DNA hybridization, we first established the capability in imaging single fluorescent molecules that were immobilized on a solid surface. In this case, surface-immobilized MBs were used to monitor the hybridization kinetics. The density of the immobilization was controlled to be low enough to enable us to isolate individual molecules in a fluorescence image. The immobilized MBs were excited by the evanescent field produced at the silica–water interface. The narrow depth of the excitation field greatly reduced the background and enabled a clear fluorescent image for the single immobilized MB molecules. A typical image (150 pixels × 160 pixels, 33 μm × 35.2 μm) of the surface-immobilized MB and an image of the same area after addition of cDNA (100 nM, at pH 8.0) are shown in Figure 2a and b, respectively. Each bright spot in the images corresponds to the fluorescent signal from one MB molecule or one MB–cDNA hybrid. These two images were displayed into 3D images (Figure 2c and 2d) for clearer presentation.

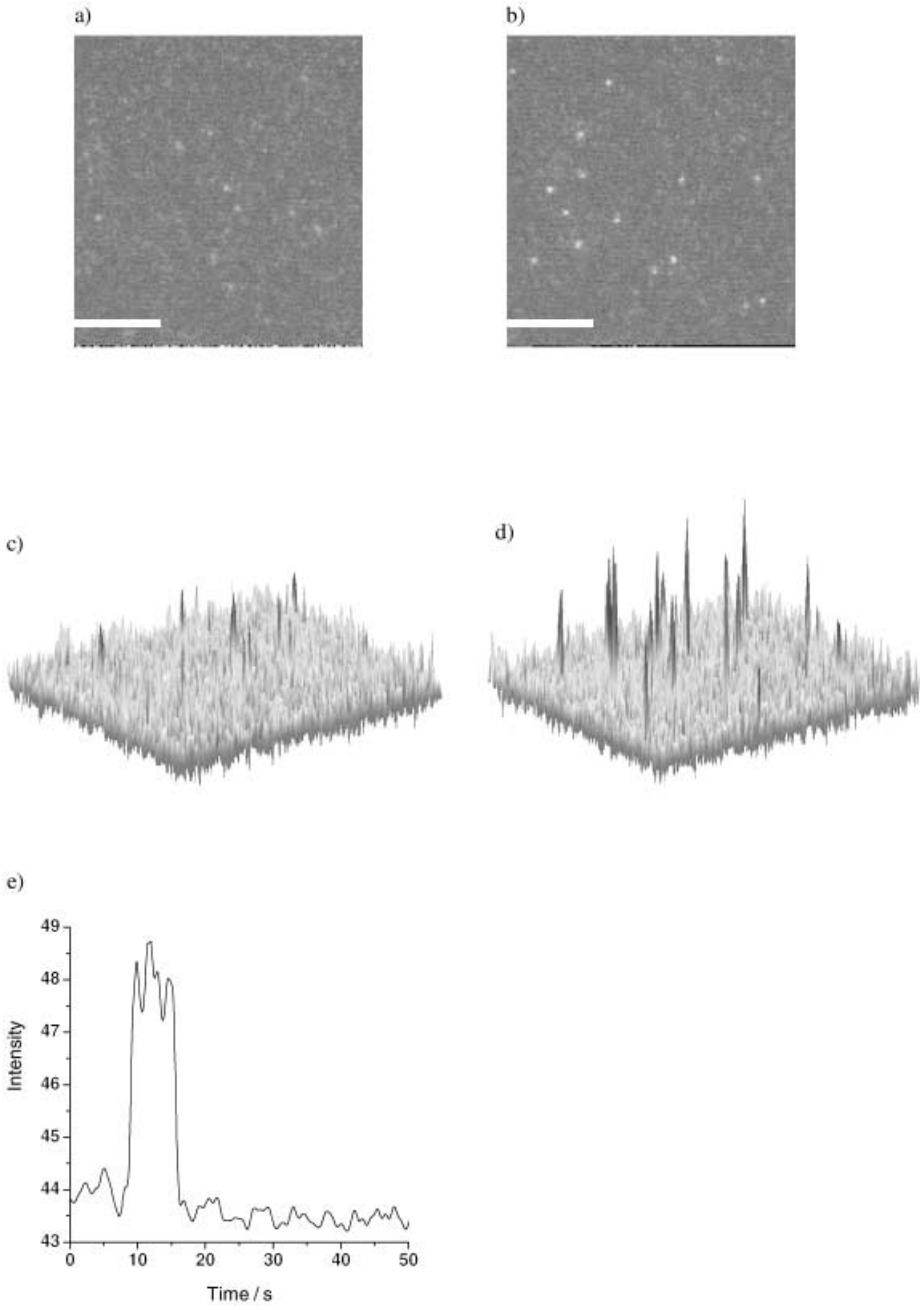

Figure 2. Fluorescence microscopy images and 3D images of the immobilized MB in the absence (a, c) and presence (b, d) of 100 nM cDNA (150 pixel × 160 pixel, scale bar: 10 μm). The typical photobleaching properties of MB–cNDA are shown in (e).

Interesting and useful information can be obtained from these images. The first observation concerns the different spatial profiles in Figure 2a and b: There are more bright spots with higher intensity in Figure 2b, which was observed after the addition of cDNA to the surface-immobilized MBs. This difference can be explained by the conformational change of the MBs before and after the hybridization with their cDNAs. In the absence of cDNA, the stem-and-loop structure keeps the fluorophore close to the quencher, causing the fluorescence quenching, and thus there are only a few bright spots with weak fluorescent intensity in Figure 2a. Upon hybridization with their cDNAs, the surface-immobilized MBs undergo a conformational reorganization that leads to the opening of the stem and the restoration of the fluorescence of the fluorophore, which is manifests itself in the more bright spots in Figure 2b. The second observation is that each bright spot in the images corresponds to a single MB molecule. The photobleaching behavior of these molecules was examined and Figure 2e shows a typical photobleaching temporal monitoring curve from the bright spots in Figure 2b. The fluorescence intensity is constant for about 7 s then suddenly drops to the background level in a one-step process. The abrupt disappearance of intensity is an indication that the fluorescence of each bright spot originates

from one single dye molecule.[1–5,7,9–13] The third observation is the photobleaching time. Although the bright spots display one-step photobleaching behavior characteristic of single molecules, we found that different bright spots had different fluorescence survival times before photobleaching. This time distribution provided us with a way to study the photochemical properties of the dye in the MB or MB–cDNA duplexes.

Imaging the process of single-molecule hybridization: The single-molecule imaging enables the elucidation of the hybridization process for individual DNA molecules. We were able to monitor the DNA hybridization process, as shown in Figure 3. A series of typical frames were obtained from a sequence of fluorescence images taken at different times after the introduction of cDNA to the immobilized MB. The progression of single MB hybridization at the interface was clearly observed. At time 0, there was almost no bright SM spot. At 3 s, three bright spots were observed, two of which disappeared within a short time, while the third one maintained a constant fluorescent intensity for a longer time. As the hybridization proceeded, the number of bright spots increased with time. Continuous excitation of the fluorescent molecules would result in the photobleaching of the dye-labeled DNA molecules. There were no molecules left after 39 s. A movie file of the hybridization process is available as Supporting Information for this paper. The hybridization dynamics of single immobilized DNA molecules can be monitored and analyzed.

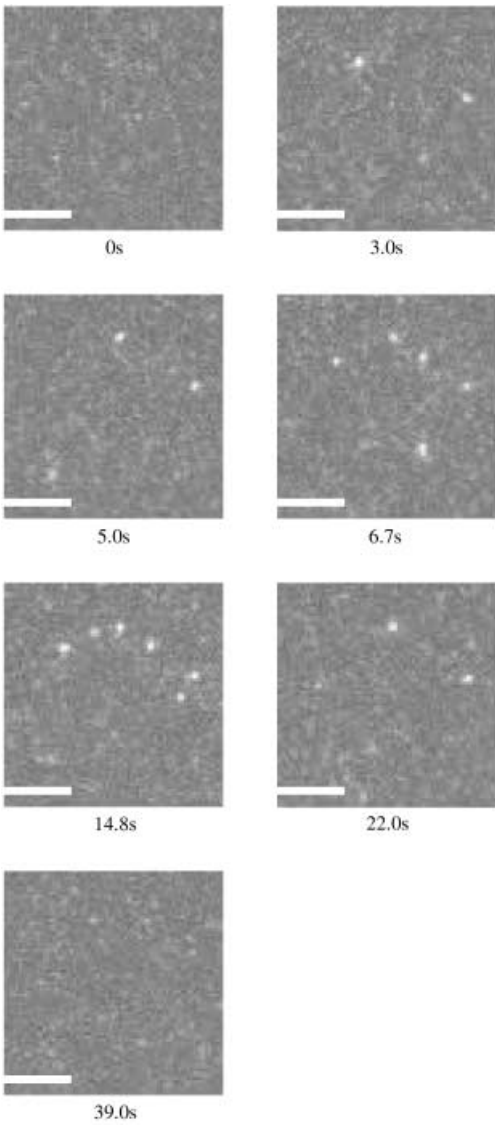

Figure 3. Fluorescence microscopy images (73 pixel × 75 pixel) of the hybridization of the immobilized MB and 100 nM cDNA during the time course of hybridization (scale bar: 5 μm).

The immobilized MB used in our experiments provided a better way to study DNA hybridization at the single-molecule level.[26,27] Using single-molecule spectroscopy, Trabesinger et al.[26] and Osborne et al.[27] have independently tried to observe the hybridization of immobilized dye-labeled DNA with its complementary DNA labeled with a dye. Both of them observed a low level of colocalized fluorescence, which was indicative of low hybridization efficiency. As studied in detail by Niemeyer et al,[28] the differences in hybridization efficiency are likely to be caused by the individual base composition of the particular oligonucleotides studied. Osborne et al. suggested that immobilized DNA had limited accessibility to the DNA in solution and the immobilized DNA had collapsed on the surface. In their work, Osborne et al immobilized 21-mer linear oligonucleotides on a glass surface by using amine/epoxide chemistry through a six-carbon-atom linker, and treated the glass with a solution of complementary oligonucletide. In our work, the linear DNA was replaced with the stem-and-loop structured MB, which was then immobilized on the biotin reactive surface through a linker of ten thymine bases. After DNA hybridization with the MB on this surface, many bright spots were obtained for dynamic analysis. We believe that the 10-thymine linker has provided surface-immobilized MB molecules with more flexibility in hybridization than those reported for linear single-stranded DNA. We also believe that the MB approach results in fewer surface-immobilized DNA molecules collapsed onto the solid surface.

Hybridization dynamics: We have studied the dynamics of the hybridization of single DNA molecules by monitoring fluorescent intensity changes. Three representative temporal curves are shown in Figure 4, which reflect the different dynamic processes of individual MB molecules in surface hybridization. Among the 400 MB–cDNA hybrid pairs we traced, 349 of them (87.5%) showed an abrupt fluorescent increase (shorter than the 100 ms temporal resolution we have with the imaging system, Figure 4a), indicating that those hybridization reactions were fast. With our current experimental set-up, we are not able to get more detailed information about the hybridization processes from those spots. Meanwhile, 51 hybrid pairs (12.5%) showed a gradual increase in fluorescence (Figure 4b and c), indicating that those MB molecules hybridized slowly with their cDNA in solution. A variety of control experiments were performed to verify this result. First, we verified that there were few bright spots on the surface when a buffer (without cDNA) solution was flowing through the channel. Second, when the

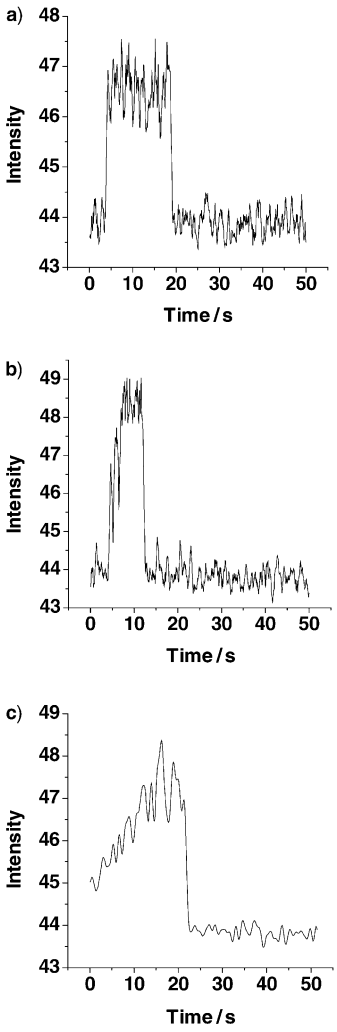

Figure 4. Dynamic curves of the hybridization of MB and cDNA observed at the single-molecule level. a) An abrupt increase of fluorescent intensity, while b) and c) show a gradual increase in fluorescence intensity.

concentration of cDNA was changed during the hybridization on the surface, the ratio of fast hybridization versus slow hybridization remained about the same, while the overall hybridization events on the surface changed. Although the cDNA solution concentration varied from 50 nM to 500 nM, it was clear that ratio did not change significantly. This result indicates that the fast hybridization and slow hybridization are mainly due to the way in which the MBs are immobilized on the silica surface.

In the slower reactions with the MB molecules, we are able to monitor the hybridization dynamics. If we define the hybridization time as the time needed for a MB molecule to increase its fluorescence from the background to the high plateau intensity, analysis of the hybridization time for those 51 gradually increased MBs yields a distribution as plotted in Figure 5. The data in the histogram fit well to a first-order exponential decay curve with a scale parameter $\tau = 5.5 \pm 0.6$ s ($\chi^2 = 1.73$, $R^2 = 0.95$). The exponential curve suggested that the hybridization of a MB with its cDNA was a Poisson process, and the average hybridization time was

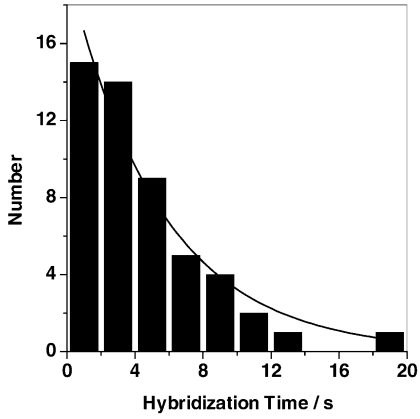

Figure 5. Histogram of the measured hybridization time of immobilized MB with its cDNA.

about 5.5 s for the slow-type hybridization. Since this pattern of change in the fluorescence intensity has neither been observed in the images of single MBs nor in the images of the MB–cDNA hybrid, the gradual increase in fluorescence should be due to the hybridization of the MB with its cDNA. It is clear that even though the majority of the MB molecules hybridized very quickly, a small portion of the MB molecules hybridized slowly. We speculate that there might be two different types of surface-immobilized MBs, one far away from the surface and the other one closer to or on the surface which hinders hybridization processes.

Photostability: We have also observed interesting photochemical properties of the MB and MB–cDNA hybrids. As we discussed before, different molecules have different photobleaching times. In the image of MB–cDNA (Figure 2b), some bright spots disappeared within several seconds, and others lasted between 10 and 40 seconds. To probe the photostability of the fluorophores in the MBs and in the MB hybrids, the photobleaching times of 290 MB–cDNA molecules were analyzed. Histograms of their photobleaching times are shown in Figure 6a, which reveals a distribution in excellent agreement with an exponential decay curve. The profiles suggest that the photobleaching of these fluorophores is a Poisson process. The regression parameters showed that MB–cDNA had an average photobleaching time of 11.2 ± 0.7 s. The same experiments were performed on 220 denatured MB molecules (the stem–loop structure was opened) and 215 TMR molecules. Their photobleaching time profiles were also found to fit a similar pattern. The average photobleaching times were 1.0 ± 0.1 s and 3.2 ± 0.3 s for denatured MB and TMR, respectively. The different photobleaching times clearly showed that the TMR dye in MB–cDNA hybrids has the highest photostability. It is worth noting that all these experiments were performed under strictly controlled experimental conditions (same laser intensity, coupling efficiency etc) to assure a fair comparison.

Our results on photobleaching times are comparable to those reported in the literatures. Wennmalm and Rigler[29] immobilized TMR-labeled 217-bp DNA on a glass surface by using the biotin–streptavidin interaction. The photobleaching time was 4.1 ± 0.5 s based on a study on 102 sur-

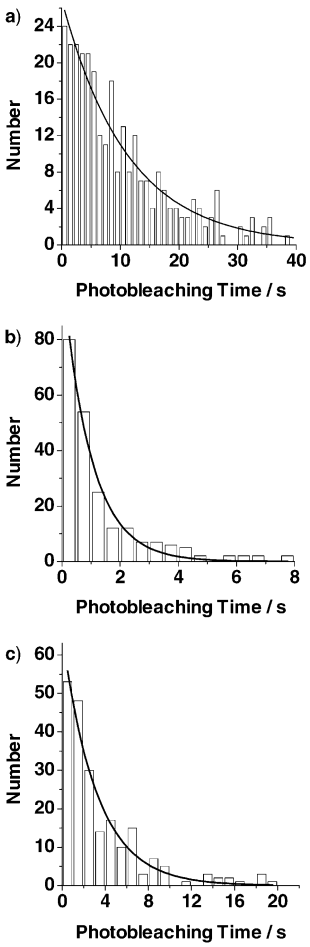

Figure 6. Histogram of photobleaching times of immobilized MB–cDNA (a), denatured MB (b), and free TMR (c).

face-attached DNA molecules with epi-fluorescence. However, in their bulk experiments (not single-molecule studies), two characteristic photobleaching times of 1.7 and 8.1 s were obtained. Similarly, Osborne[27] analyzed the photobleaching times of over 1300 covalently immobilized TMR-labeled DNA molecules, and found two components (3.5 and 15.7 s) in the average photobleaching times. Photobleaching time gives information about the local environment of the fluorophore. Both experiments indicated that there are two components of photobleaching time for the interconversion of TMR molecules between two different environments. Since they only got one regressive photobleaching time in their single-molecule study, Wennmalm and Rigler also believed these 102 selected molecules were in the same environments during the imaging time. In our experiments, we have one photobleaching time for each kind of dye molecule. All three photobleaching times fitted well to a first-order exponential decay curve, indicating that the dye molecules were in the same environment in their corresponding samples during the measurements. However, these environments are different in different samples.

Photobleaching is the result of a photo-related reaction of the dye molecules with the surrounding molecules, resulting in photodestruction of the dye. The easier the reaction is, the shorter the photobleaching time will be. There were two possible factors that might influence the photobleaching time: the effect of the quencher and the structure of DNA. The denatured MB has a fluorescent intensity very similar to that for the MB–cDNA hybrid, which means the quencher of the denatured MB is far away from the fluorophore and thus has little effect on the properties of the fluorophore. On the other hand, the denatured MB is a single-stranded DNA, while the MB–cDNA is double-stranded. The microenvironments of the dye are not the same. We speculate that the close proximity to the double-stranded structure might protect the fluorophores and thus results in a longer photobleaching time for the MB hybrid than for the denatured MB.

Hybridization mechanism: Theoretically, the formation of a DNA duplex is a multistep reaction, and each base-pairing step has a different reaction constant. Analysis of the hybridization process is complicated in this mode. A much simpler mode, all-or-none mode, an approximation that only considers the initial and final states of a reaction, has been proposed.[30] This mechanism has been found to be sufficient to explain most of the kinetic experimental data and is widely accepted for DNA hybridization studies. The all-or-none mode is supported by the results of a thermodynamic study of bulk MB hybridization.[31]

If we only consider the initial and final states, the all-or-none mode could explain our data for the 87.5 % of the molecules. However, we also had 12.5 % of the MB molecules that appeared to exhibit a gradual increase and these could not be explained by the all-or-none mode. We think that the conformational change of the MB from the stem-closed state to the open state happens synchronously with the process of the hybridization. It is well known that the kinetics of the conformational fluctuation of a DNA hairpin-loop itself is very fast. The open and closed transition in the MB has been reported in μs range.[32] With the 100 ms exposure time in our experiments, the MB may experience several cycles of conformational change, and spend n (n is just a parameter) ms in the open state and $(100-n)$ ms in the closed state. If the MB in the closed state has a weak fluorescent intensity, F_1, and a strong intensity, F_2, in the open state, what we observe is the average intensity of the open state and the closed state $(((100-n)F_1+nF_2)/100)$. When the MB is in its open state, the fluorescent intensity should be similar to that of the MB duplex. After the MB changed to its open state, the hybridization started at a single base-pairing, then the number of the base-pairings increased until full matching was achieved between the MB and the target. During this hybridization process, the MB, which is coupled with the target through one or more bases, is still in equilibrium between the open and closed state. However, changing from the open state to the closed state becomes harder. The more base-pairing between the MB and cDNA resulted in a longer duration time of the open state (n ms) for the MB in every 100 ms exposure time, contributing to an increase of the average fluorescent intensity $((100-n)F_1+nF_2)/100$. The average fluorescence of the MB in 100 ms (exposure time) thus increases gradually as more and more bases become paired. If the hybridization time is shorter than our 100 ms

exposure time, we could only observe an abrupt fluorescent increase for 87.5% of the molecules. When it takes longer than 100 ms for the MB to fully hybridize its cDNA, we would find a gradual increase in the curve for the hybridization process as presented by 12.5% of the molecules. We also believe that if the exposure time is shorter than 100 ms, we may observe more MB molecules showing a gradual increase.

The hybridization process of surface-immobilized DNA with its cDNA is complicated. Although most of the observed reactions do not provide us with more detailed information about the hybridization process, statistical data of the 51 single-molecule hybridization images showed that there might be a multistep reaction and hybrid intermediates. The study of the MB hybridization at the single-molecule level thus enables us a better understanding of the hybridization mechanism. It is expected that the new understanding of the MB hybridization process will help in our MB-based biosensor and biochip development where surface-immobilized MBs are used for gene target elucidation.

Conclusion

Herein, we have studied the hybridization dynamics of molecular beacon DNA probes at the single-molecule level. For the first time, we have monitored the dynamic process of the hybridization of single DNA molecules at a solid/liquid interface in real-time. The surface-immobilized molecular beacons show two major types of kinetics during their hybridization: fast dynamics for 87.5% of the molecular beacon DNA probes and slow dynamics for 12.5% of the molecular beacon probes. This result is further confirmed by control experiments and by the results obtained when cDNA concentrations were varied during the monitoring of the hybridization at the surface/liquid interface. We also found that the fluorophores in newly formed double-stranded hybrids are much more stable optically than those of the denatured single-stranded molecular beacon DNA probes. Our single-molecule studies provide a new means to understand the DNA hybridization mechanism at solid/liquid interfaces, and will be highly useful for the elucidation of biomolecular reactions and interactions at an interface. The better understanding of the hybridization dynamics will improve biosensor and biochip development where surface-immobilized molecular beacon DNA probes provide unique advantages in signal transduction.

Acknowledgement

This work is partially supported by NIH NCI CA92581 and R01 GM66137–01, by Cottrell Scholar program from Research Corporation and by Packard Foundation Science and Technology Award.

[1] W. E. Moerner, L. Kador, *Phys. Rev. Lett.* **1989**, 62, 2535.
[2] T. Funatsu, Y. Harada, M. Tokunaga, K. Saito, T. Yanagida, *Nature* **1995**, 374, 555.
[3] S. Nie, R. N. Zare, *Annu. Rev. Biophys. Biomol. Struct* **1997**, 26, 567.
[4] X. S. Xie, J. K. Trautman, *Annu. Rev. Phys. Chem.* **1998**,49,441.
[5] R. M. Dickson, D. J. Norris, Y. L. Tzeng, W. E. Moerner, *Science (Washington, D.C.)* **1996**, 274, 966.
[6] X. Xu, E. S. Yeung, *Science* **1997**, 275, 1106.
[7] P. Zhang, W. Tan, *Chem. Eur. J.* **2000**, 6, 1087.
[8] M. Ueda, Y. Sako, T. Tanaka, P. Devreotes, T. Yanagida, *Science (Washington, D.C.)* **2001**, 294, 864.
[9] H. Bayley, O. Braha, L. Gu, *Adv. Mater.* **2000**, 12, 139.
[10] O. Braha, L. Gu, X. Lu, S. Cheley, H. Bayley, *Nature Biotech.* **2000**, 18, 1005.
[11] S. Weiss, *Science* **1999**, 283, 1676.
[12] C. Bustamante, S. B. Smith, J. Liphard, D. Smith, *Curr. Opin. Struc. Biol.* **2000**, 10, 279.
[13] T. Ha, *Curr. Opin. Struc. Biol.* **2001**, 11, 287.
[14] J. Wang, P. Wolynes, *Phys. Rev. Lett.* **1995**,74,4317.
[15] L. Edman, U. Mets, R. Rigler, *Proc. Natl. Acad. Sci. USA* **1996**, 93, 6710.
[16] S. H. Kang, M. R. Shortreed, E. S. Yeung, *Anal. Chem.* **2001**, 73, 1091.
[17] X. Fang, W. Tan, *Anal. Chem.* **1999**, 71, 3101.
[18] S. Tyagi, F. R. Kramer, *Nat. Biotechnol.* **1996**, 14, 303.
[19] X. Fang, J. Li, J. Perlette, K. Wang, W. Tan, *Anal.Chem.* **2000**, 72, 747A-753A; J. Perlette, W. Tan, *Anal. Chem.* **2001**, 73, 5544–5550.
[20] T. Matsuo, *Biochim. Biophys. Acta* **1998**, 1379, 178.
[21] X. Fang, X. Liu, S. Schuster, W. Tan, *J. Am. Chem. Soc.* **1999**, 121, 2921.
[22] J. Li, X. Fang, S. Schuster, W. Tan, *Angew. Chem.* **2000**, *112*, 1091; *Angew. Chem. Int. Ed.* **2000**, 39, 1049.
[23] W. Tan, X. Fang, J. Li, X. Liu, *Chem. Eur. J.* **2000**, 6, 1107.
[24] Y. Miyamoto, E. Muto, T. Mashimo, A. H. Iwane, I. Yoshiya, T. Yanagida, *Biophys. J.* **2000**, 78, 940.
[25] E. J. G. Peterman, S. Brasselet, W. E. Moerner, *J. Phys. Chem. A* **1999**,103, 10553.
[26] W. Trabesinger, G. J. Schutz, H. J. Gruber, H. Schindler, T. Schmidt, *Anal. Chem.* **1999**, 71, 279.
[27] M. A. Osborne, C. L. Barnes, S. Balasubramanian, D. Klenerman, *J. Phys. Chem. B* **2001**, 105, 3120.
[28] C. M. Niemeyer, W Burger, R. M. J. Hoedemakers, *Bioconjug. Chem.* **1998**, 9, 168
[29] S. Wennmalm, R. Rigler, *J. Phys. Chem. B* **1999**, 103, 2516.
[30] C. R. Cantor, P. R. Shimmel, *Biophysical chemistry: They behavior of biological macromolecules, part III,* Freeman, San Francisco, **1980**, pp. 1109–1264.
[31] G. Bonnet, S. Tyagi, A. Libchaber, F. R. Kramer, *Proc. Natl. Acad. Sci. USA.* **1999**, 96, 6171.
[32] G. Bonnet, O. Krichevsky, A. Libchaber, *Proc. Natl. Acad. Sci. USA.* **1998**, 95, 8602.

Received: March 23, 2003 [F4977]